Inorganic Chemistry

ARTICLE

pubs.acs.org/IC

Liquid−Liquid Biphasic Synthesis of Layered Zinc Hydroxides Intercalated with Long-Chain Carboxylate Ions and Their Conversion into ZnO Nanostructures

Sara Inoue and Shinobu Fujihara*

Department of Applied Chemistry, Keio University, 3-14-1 Hiyoshi, Kohoku-ku, Yokohama 223-8522, Japan

Supporting Information

ABSTRACT: A method for synthesizing layered zinc hydroxide compounds in high yields is developed using an immiscible liquid−liquid system in one pot. Long-chain carboxylate ions such as heptanoate, decanoate, and dodecanoate were successfully intercalated between zinc hydroxide layers in one process starting from a xylene−water system. Typically, a xylene phase dissolving the respective carboxylic acids was allowed to stand in contact with an aqueous phase dissolving zinc nitrate hexahydrate and urea. During keeping the resultant biphasic system at 80 °C, urea was thermo-hydrolyzed to supply OH^- in the aqueous phase while the carboxylic acids were continuously transferred from the xylene phase under the distribution law. The aqueous phase was then supersaturated, and a solid phase of layered basic zinc carboxylate was precipitated as films on glass substrates through heterogeneous nucleation and subsequent two-dimensional crystal growth. Crystal structures and morphology of the films were modulated by the kind of the carboxylic acids employed. The layered basic zinc carboxylate films could be converted to nanostructured, mesoporous ZnO films by heating at 450 °C in air. The relationship between the initial solution compositions and the final solid products was systematically examined to discuss reaction mechanisms in the biphasic systems.

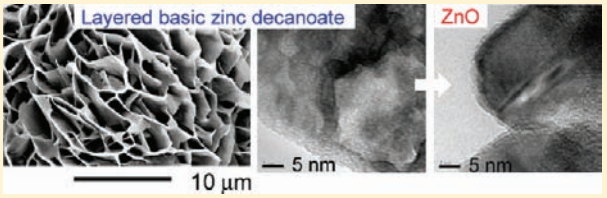

INTRODUCTION

Layered metal hydroxide compounds have attracted much attention as multifunctional materials for anion exchange,[1] intercalation,[2] catalysis,[3] two-dimensionally confined reaction space,[4] and exfoliation to nanosheets[5] due to their characteristic lamellar structure. Among them, layered basic metal salts (LBMSs) with a general formula of $[M^{2+}(OH)_{2-x}]A^{n-}{}_{x/n}\cdot mH_2O$, where M^{2+} is a divalent metal ion in the octahedral site of brucite-type hydroxide layers and A^{n-} is an interlayered anion to keep a whole charge balance, are recognized as a new class of hybrid precursors that can be thermally decomposed into single metal oxides such as CuO,[6] NiO,[7] and Co_3O_4.[8] We have been focusing on layered basic zinc salts (LBZSs) with a general formula of $Zn(OH)_{2-x}A^{n-}{}_{x/n}\cdot mH_2O$ (A^{n-} = Cl^-, NO_3^-, CO_3^{2-}, CH_3COO^-, etc.). LBZSs with the lamellar structure are indeed promising as precursors for fabricating two-dimensionally (2D) structured, mesoporous ZnO materials with high specific surface areas,[9] which otherwise might not be formed by direct crystal growth of wurtzite-type ZnO with a general tendency of having one-dimensional (1D) structures.[10] ZnO is an n-type semiconductor with a wide and direct band gap, a large exciton binding energy, and high electronic mobility. In particular, ZnO having high surface areas are required in physicochemical and electrochemical applications including gas sensors,[11] photocatalysts,[12] and photoanodes.[13] It has been reported that the 2D sheet-like morphology of LBZSs can be varied depending on kinds of the interlamellar species intercalated into the brucite-type layers.[14] It is therefore a challenging undertaking to intercalate a variety of hydrophilic or hydrophobic organic species between the zinc hydroxide layers.

Recently, we proposed the utilization of immiscible liquid−liquid biphasic systems for the synthesis of LBZSs intercalated with hydrophobic organic species. In our first report,[15] we examined a system where hydrophobic benzoic acid (C_6H_5-COOH) was dissolved in an organic phase and building blocks of zinc hydroxide layers (Zn^{2+} and OH^-) were in an aqueous phase. Our synthesis method is based on the principle of the distribution equilibrium of solutes between two liquid phases. Benzoic acid could then be continuously delivered from the organic phase to the aqueous phase to form crystalline solid precipitates (layered basic zinc benzoate; LBZB) by getting supersaturated, accompanying a gradual release of OH^- by thermal decomposition of urea added to the aqueous phase. Additionally, the LBZB compound could be deposited on glass substrates as 2D-structured uniform films by controlling the heterogeneous nucleation and subsequent crystal growth.

The LBZS compounds have been synthesized so far using typically the single liquid-phase media with precipitation,[16] anion exchange,[2] reconstruction of metal oxides or hydroxides,[14,17] chimie douce method,[18] chemical bath deposition,[9,19] or cathodic deposition.[20] Unlike these single-phase systems, the biphasic

Received: December 26, 2010
Published: March 24, 2011

Table 1. Carboxylic Acids Employed in the Present Work and Their Concentration in the Organic Phase[a]

carboxylic acid	chemical formula	examined concentration/ mol·dm^{-3}	optimized concentration/ mol·dm^{-3}	yield (%)
benzoic acid	C_6H_5COOH	0−0.6	0.1	88.8
heptanoic acid	$CH_3(CH_2)_5COOH$	0−0.6	0.1	69.8
decanoic acid	$CH_3(CH_2)_8COOH$	0−0.6	0.4	63.2
dodecanoic acid	$CH_3(CH_2)_{10}COOH$	0−0.6	0.3	60.2

[a] A yield was calculated for the respective layered basic zinc salts that were obtained by optimizing the concentration of the carboxylic acids.

liquid−liquid system is expected to be capable of producing much higher yields of LBZSs in one pot and one process without specialized equipment, due to the continuous transport of hydrophobic organic species through the liquid−liquid interface. In the present work, we successfully introduced biphasic xylene−water systems to the synthesis of a new family of LBZSs intercalated with various hydrophobic long-chain carboxylate ions such as heptanoate ($CH_3(CH_2)_5COO^-$), decanoate ($CH_3(CH_2)_8COO^-$), and dodecanoate ($CH_3(CH_2)_{10}COO^-$). The LBZSs intercalated with these carboxylate ions could be obtained in the biphasic systems as 2D-structured dense films on glass substrates. They exhibited unique crystal structures and morphologies because of different molecular structures, distribution ratios, and acid dissociation constants of the carboxylic acids employed. Conversion of the resultant LBZS films into ZnO was also investigated.

EXPERIMENTAL SECTION

Synthesis. Zinc nitrate hexahydrate ($Zn(NO_3)_2\cdot 6H_2O$, 99.0% purity, Wako Pure Chemicals Co., Ltd., Japan) and urea ($(NH_2)_2CO$, 99.0%, Wako) were dissolved in deionized water with the assistance of ultrasonication at room temperature. Separately, benzoic acid (C_6H_5COOH, 99.5%, Wako), heptanoic acid ($CH_3(CH_2)_5COOH$, 98.0%, Wako; also known as enanthic acid), decanoic acid ($CH_3(CH_2)_8COOH$, 98.0%, Wako; capric acid), and dodecanoic acid ($CH_3(CH_2)_{10}COOH$, 98.0%, Wako; lauric acid) were dissolved in xylene as well. Benzoic acid, as one of the aromatic carboxylic acids, was used for a comparative study against the long-chain carboxylic acids. Concentrations of Zn^{2+} and urea in aqueous solution were fixed at 0.1 and 1.0 mol/dm^3, respectively, while those of the carboxylic acids in the organic solutions were varied between 0 and 0.6 mol/dm^3 (see Table 1). A 7 mL amount of the xylene solution was injected gently onto an equal volume of the aqueous solution using a syringe, keeping disturbance minimal. The resultant solutions were biphasically separated and maintained at 80 °C for 24 h in a dry block bath without stirring. It was observed that a solid phase was formed preferentially on the internal wall of a glass container in the aqueous phase through heterogeneous nucleation and subsequent crystal growth.

The deposition of films was then expected in a controlled manner by using a certain kind of flat substrates. We chose soda-lime glass slides 1 mm in thickness in the present work because they could provide the flat surface. For a specific application, other kinds of substrates such as transparent conductive glass plates would also be utilized. The soda-lime glass slides were put into bottles filled with the biphasically separated solutions to contact only with the aqueous phase. After the deposition at 80 °C for 24 h, the film samples obtained were dried under ambient condition. We used the deposits on the substrate surface facing the bottom of the container for the following characterization. In some cases, however, solids were also formed in the organic phase after being cooled to room temperature, depending on the initial concentrations of the carboxylic acids. Such samples were collected after being isolated and dried under ambient condition. The film samples were finally heat treated at 450 °C for 1.5 h in air to be converted to ZnO.

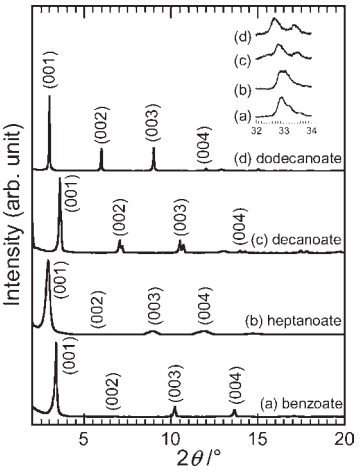

Figure 1. XRD patterns of film samples deposited in the aqueous phase in the presence of (a) benzoate, (b) heptanoate, (c) decanoate, and (d) dodecanoate ions. (Inset) Magnification of the 2θ range between 32° and 34°.

Characterization. The crystal structure of the samples was identified by X-ray diffraction (XRD) analysis with a Bruker AXS (Japan) D8 ADVANCE diffractometer using Cu Kα radiation (λ = 1.5405 Å). To examine the layered structure of the samples, the $\theta-2\theta$ scan was started from a low diffraction angle of θ = 1°. The organic species present in the samples were examined by Fourier transform infrared (FT-IR) spectroscopy with a Varian Technologies (Japan) FTS-60A/896 spectrometer using a KBr method. The sample morphology was observed by field emission scanning electron microscopy (FE-SEM) with a Hitachi (Japan) S-4700 and an FEI (USA) Sirion microscope. The microstructure was observed by transmission electron microscopy (TEM) with a Philips (The Netherlands) TECNAI F20 microscope. The thermal decomposition behavior of the samples was examined by thermogravimetry-differential thermal analysis (TG-DTA) with a Mac Science (Japan) 2020S analyzer using a heating rate of 2 °C/min in flowing air. The specific surface area of the samples was determined by the Brunauer−Emmett−Teller (BET) method based on the nitrogen adsorption isotherm at 77 K with a Shimadzu (Japan) Tristar 3000 micrometric analyzer. For XRD, FT-IR, TG-DTA, and BET measurements, the film samples were removed from the substrate by scratching and treated as powdery samples.

RESULTS AND DISCUSSION

XRD. Under the distribution law of solutes between two immiscible liquid phases, a small amount of carboxylic acid (RCOOH) is transferred from the organic to the aqueous phase and is partially dissociated into a carboxylate ion ($RCOO^-$) and a proton. Figure 1 shows XRD patterns of film samples deposited in the aqueous phase in the presence of the respective carboxylate ions delivered from the organic phase. The concentrations of the carboxylic acids in the initial xylene solutions were preliminarily

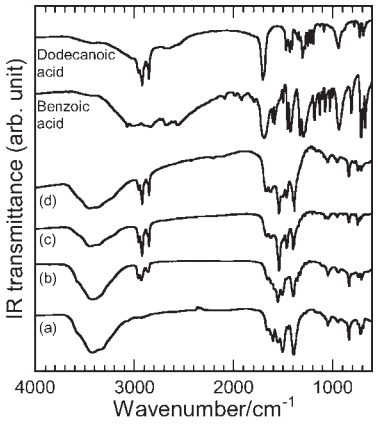

Figure 2. FT-IR spectra of the film samples deposited in the aqueous phase in the presence of (a) benzoate, (b) heptanoate, (c) decanoate, and (d) dodecanoate ions. Spectra of benzoic and dodecanoic acid are also shown for comparison.

optimized to 0.1, 0.1, 0.4, and 0.3 mol/dm^3 for benzoic, heptanoic, decanoic, and dodecanoic acid, respectively, to give the highest yields (Table 1). It is seen from the figure that all of the samples show the respective XRD patterns typical of the layered structure with stronger peaks appearing in the lower 2θ range. The patterns exhibit equally spaced peaks with d values (d = the spacing between diffracting planes) of 26.15 (2θ = 3.38°), 13.00 (6.80°), 8.64 (10.23°), and 6.48 Å (13.66°) for the sample obtained in the presence of the benzoate ions, 30.20 (2θ = 2.93°), 15.31 (5.77°), 9.90 (8.93°), and 7.42 Å (11.92°) for the heptanoate ions, 25.30 (2θ = 3.49°), 12.73 (6.95°), 8.50 (10.41°), and 6.38 Å (13.88°) for the decanoate ions, and 29.69 (2θ = 2.98°), 14.77 (5.98°), 9.83 (8.99°), and 7.37 Å (12.01°) for the dodecanoate ions. These diffraction peaks can be indexed as (00l) planes of the layered structure. As shown in an inset of Figure 1, broad and asymmetric peaks at d = 2.72 (2θ = 32.93°), 2.71 (33.00°), 2.73 (32.75°), and 2.74 Å (32.69°) for the benzoate, heptanoate, decanoate, and dodecanoic ions, respectively, are attributed to the (100) plane commonly found in any other LBZSs with the brucite-type zinc hydroxide structure.[18] A close look at the patterns around 2θ = 33° reveals that shoulder peaks appear at d = 2.68 Å (33.41° and 33.43°) for the decanoate and dodecanoate ions, respectively. A detailed interpretation of these minor peaks will be made later. The above XRD data indicate that the film samples have almost the same brucite-type zinc hydroxide layers with different basal spacings depending on the kind of the carboxylate ions present in the biphasic systems.

FT-IR and TG-DTA. In our biphasic systems, there exist four possible species that can be intercalated, namely, the carboxylate, nitrate (NO_3^-), and carbonate (CO_3^{2-}) ions derived from the starting carboxylic acids, zinc nitrate ($Zn(NO_3)_2 \cdot 6H_2O$), and urea ($(NH_2)_2CO$), respectively, and the water molecules in the aqueous phase. Urea in the aqueous solution is thermo-hydrolyzed to form ammonia and carbon dioxide, which react with water to produce OH^- and CO_3^{2-}, respectively.[19] We then attempted to distinguish these species by FT-IR spectroscopy and TG-DTA analysis.

FT-IR spectra of the film samples deposited in the aqueous phase together with those of benzoic and dodecanoic acid as references for carboxylic acids are compared in Figure 2. At a higher wavenumber range, intense and broad absorption bands are observed between 3650 and 3100 cm^{-1} for all the film samples, resulting from the stretching vibration mode of the hydroxyl group (−O−H) of the crystallization water and the zinc hydroxide layers ($Zn(OH)_x$). In the spectra of benzoic and dodecanoic acid, weaker and broader absorptions detected between 3200 and 2500 cm^{-1} can be assigned to the stretching vibration mode of "−O−H" in the carboxyl group. The "$-CH_2-$" methylene groups of the linear-chain carboxylic acids are evidenced by three characteristic bands at 2954, 2920, and 2845 cm^{-1} for the samples deposited in the aqueous phase in the presence of the heptanoate, decanoate, and dodecanoate ions and also for pure dodecanoic acid, arising from the "−C−H" stretching vibration mode. At a lower wavenumber range, the "C═C" stretching vibration mode of the aromatic ring is detected in the sample for the benzoate ions as a signal at 1598 and 1501 cm^{-1}. The "−C−H" antiplane bending mode of the aromatic ring is also detected at 710 and 683 cm^{-1}. The intense absorption band is observed at 1704 cm^{-1} due to the "C═O" stretching vibration mode of a neutral carboxylic acid molecule for benzoic and dodecanoic acid, while this band is completely absent for all film samples. Instead, the respective carboxylate ions display two absorption bands at 1540 and 1383 cm^{-1} resulting from the "COO^-" asymmetric and the symmetric stretching mode, respectively, in the spectra of all the samples. In addition, weak bands at 1670 and 1622 cm^{-1} for each sample can be assigned to the "−O−H" bending mode of water. Although the absorption band of NO_3^- intercalated between the brucite layers generally appears at near 1380 cm^{-1} due to the asymmetric "N−O" stretching vibration mode,[21] this band is hidden by the intense signal of the "COO^-" symmetric stretching mode of the carboxylate ions in the spectra of our samples. On the other hand, CO_3^{2-} incorporated into crystalline materials shows typically two split bands around 1500 and 1390 cm^{-1} (the asymmetric "C−O" stretching mode) and a strong single band at 835 cm^{-1} (the out-of-plane "OCO" bending mode).[22] In the spectra of our samples, the latter signal is detected for all the samples. FT-IR analysis then shows that the samples deposited in the aqueous phase of the xylene−water biphasic systems include the respective carboxylate ions, the water molecules, and the carbonate ions. The samples with the long-chain carboxylic acids can then be designated as layered basic zinc heptanoate (LBZH), layered basic zinc decanoate (LBZD), and layered basic zinc dodecanoate (LBZDd).

The thermal decomposition behavior of the film samples deposited in the aqueous phase was examined by TG-DTA analysis conducted in flowing air. As shown in Figure 3, a first gradual weight loss is observed at temperatures up to 120 °C in TG curves for all samples due to release of water intercalated into or adsorbed onto the brucite-type zinc hydroxide layers. A second weight loss occurs around 203 and 162 °C for the benzoate (Figure 3a) and the heptanoate (Figure 3b), respectively, accompanied by strong endothermic peaks. This is attributed to dehydration of the zinc hydroxide layers, as evidenced by disappearance of the (00l) peaks and appearance of new peaks indexed as hexagonal wurtzite-type ZnO (ICDD 36-1451) in XRD patterns of the samples heated at the corresponding temperatures (see Figure S1, Supporting Information). For the decanoate (Figure 3c) and dodecanoate (Figure 3d), the second weight loss with the endothermic peak is divided into two steps around 122 and 170 °C (decanoate) and 130 and 184 °C (dodecanoate). As discussed later, this two-step dehydration is related to the appearance of the shoulder peaks of the (100) plane in the XRD patterns for the decanoate and the dodecanoate

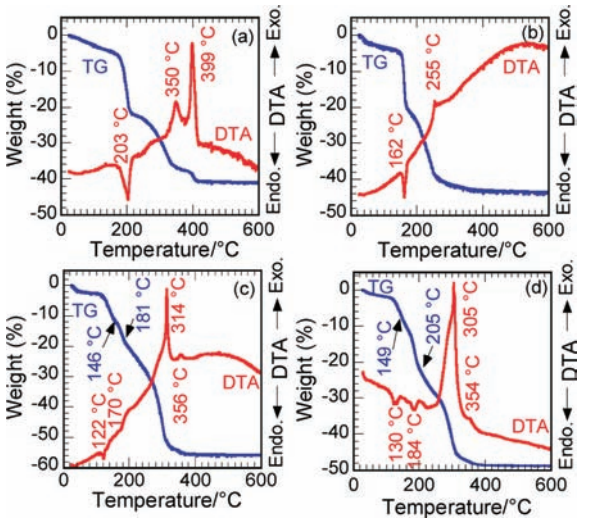

Figure 3. TG-DTA curves for the film samples deposited in the aqueous phase in the presence of (a) benzoate, (b) heptanoate, (c) decanoate, and (d) dodecanoate ions.

shown in Figure 1. Additionally, in the second weight loss, release of the carbonate ions simultaneously occurs, as revealed by the disappearance of the absorption band for the carbonate ions in FT-IR spectra of the samples heated at the corresponding temperatures (see Figure S2, Supporting Information). The carbonate ions intercalated into the zinc hydroxide layers are released generally in the temperature range of 180−250 °C in layered basic zinc carbonate (LBZC).[19] The lower releasing temperatures of the carbonate ions in the present samples indicate that the carbonate ions are not intercalated into the brucite-type layers but adsorbed on the surface in our samples. Third and fourth weight losses with exothermic peaks appear around 350 and 399 (benzoate), 255 (heptanoate), 314 and 356 (decanoate), and 305 and 354 °C (dodecanoate). These behaviors can be explained by the decomposition and oxidation of the carboxylate groups into CO_2 and H_2O in air, as confirmed by the FT-IR spectra (see also Figure S2, Supporting Information). The decomposition temperatures of the carboxylate ions incorporated in our samples are much higher than those of the corresponding carboxylic acids: 184, 165, 186, and 223 °C for benzoic, heptanoic, decanoic, and dodecanoic acid, respectively. This result suggests that the respective carboxylate ions are well stabilized by being intercalated into the zinc hydroxide layers.

On the basis of the above interpretation of the XRD, FT-IR, and TG-DTA results, approximate chemical compositions of the film samples deposited in the aqueous phase were determined to be $Zn(OH)_{1.74}(C_6H_5COO)_{0.26}\cdot 0.29H_2O$ (LBZB), $Zn(OH)_{1.73}(C_6H_{13}COO)_{0.27}\cdot 0.44H_2O$ (LBZH), $Zn(OH)_{1.58}(C_9H_{19}COO)_{0.42}\cdot 0.40H_2O$ (LBZD), and $Zn(OH)_{1.79}(C_{11}H_{23}COO)_{0.21}\cdot 0.24H_2O$ (LBZDd) for the respective carboxylate ions. A yield was calculated based on the Zn content in the sample and in the initial solution. The Zn content in the sample was determined from the weight of ZnO obtained by heating the sample. Yields of our LBZSs intercalated with the hydrophobic carboxylate ions through the liquid−liquid synthesis were found to be relatively high: 88.8%, 69.8%, 63.2%, and 60.2% for the benzoate, heptanoate, decanoate, and dodecanoate, respectively (Table 1).

Microstructural Analysis. The morphology of our LBZS film samples was observed with FE-SEM. Figure 4 shows FE-SEM

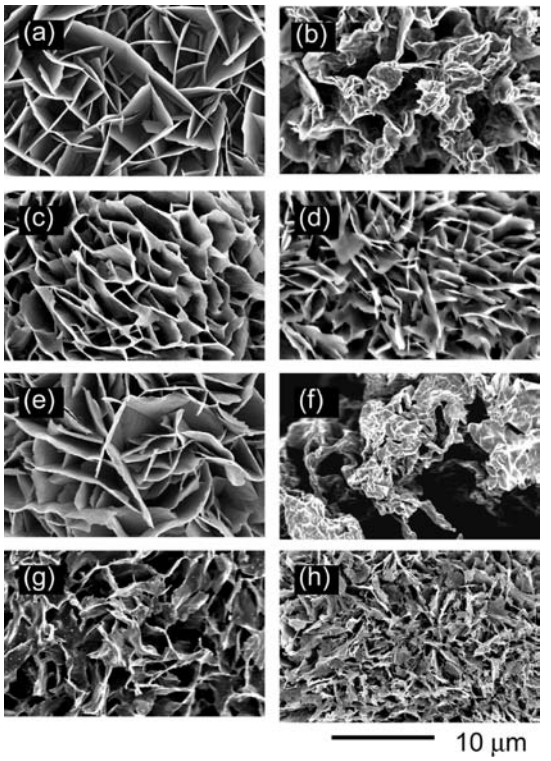

Figure 4. FE-SEM images of (a−d) the as-prepared and (e−h) heated LBZS films intercalated with (a and e) benzoate, (b and f) heptanoate, (c and g) decanoate, and (d and h) dodecanoate ions. All films were deposited on the substrate facing the bottom of the container in the aqueous phase and heat treated at 450 °C for 1.5 h in air.

images of the as-prepared and the heat-treated LBZS films intercalated with the respective carboxylate ions. All films were deposited on glass substrates facing the bottom of the container in the aqueous phase and then heat treated at 450 °C for 1.5 h in air. We reported previously that in the LBZB (benzoate) films, 2D plate-like particles composed of stacked LBZB nanosheets were first growing radically in the vertical direction and then standing upright on the substrate.[15] In the present study, the LBZS films covering completely the substrate surface have different 2D sheet-like morphology depending on the kind of the intercalated carboxylate ions. The LBZB (benzoate, Figure 4a) and LBZDd (dodecanoate, Figure 4d) film consist of planar 2D sheet-like particles. As for the LBZH (heptanoate, Figure 4b) film, 2D particles are characterized with randomly stacked and bending nanosheets having a relatively rough surface. The LBZD (decanoate, Figure 4c) film has a honeycomb structure with interconnected nanosheets. Additionally, all films are constructed with micrometer-order porous structures with different sizes of empty spaces among the respective nanosheets. After heating the LBZS films at 450 °C, they were converted to wurtzite-type ZnO (see Figure S1, Supporting Information) and underwent a small degree of volume contraction (Figure 4e−h). The heat-treated LBZH film (Figure 4f) shows crack formation arising from a significant volume contraction, whereas the LBZB (Figure 4e), LBZD (Figure 4g), and LBZDd (Figure 4h) films maintain their original 2D sheet-like morphologies after heat treatment.

The microstructural feature of the respective LBZS nanosheets, together with the effect of heat treatment, was examined by the TEM observation. Figure 5a−d shows TEM images of the

dx.doi.org/10.1021/ic1025729 |Inorg. Chem. 2011, 50, 3605–3612

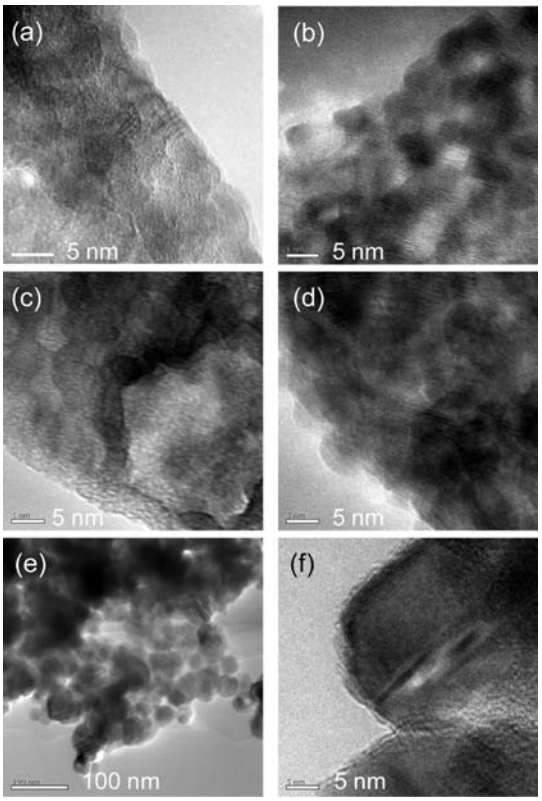

Figure 5. TEM images of nanosheets in the as-prepared LBZS films intercalated with (a) benzoate, (b) heptanoate, (c) decanoate, and (d) dodecanoate ions, and (e and f) those of ZnO converted from the LBZD shown in the panel c by heating.

as-prepared LBZS nanosheets intercalated with the respective carboxylate ions. For all samples, well-defined crystallites, typically 5 nm in size, are observed with clear lattice fringes, indicative of a polycrystalline nature of the nanosheets. Figure 5e and 5f shows TEM images of ZnO derived from the LBZD (decanoate) film by heating at 450 °C for 1.5 h in air. The heated ZnO sample has a mesoporous structure consisting of single-crystalline nanoplatelets 20−60 nm in diameter. In addition, the 2D-structured morphology of the as-prepared LBZD nanosheets is maintained after heating.

BET specific surface areas of the as-prepared LBZS film samples were measured to be 1.64, 9.52, and 7.36 m^2/g for the benzoate, decanoate, and dodecanoate, respectively. After converting to ZnO by heating, the specific surface areas were increased to 13.58 (the benzoate), 15.41 (the decanoate), and 15.61 m^2/g (the dodecanoate). On the other hand, the specific surface area of the heated ZnO sample (8.39 m^2/g) was much smaller than that of the as-prepared film sample (28.12 m^2/g) for the heptanoate, probably because of the significant volume contraction after heat treatment, as seen in Figure 4f. From the morphological and microstructural characterization, it is concluded that the LBZS films intercalated with the benzoate, decanoate, and dodecanoate ions can be converted to the 2D-structured ZnO films with specific surface areas 8.3, 1.6, and 2.1 times, respectively, larger than those of the initial LBZS films without the morphological change.

Reaction Mechanisms. In our liquid−liquid synthesis method, the distribution and dissociation behavior of the carboxylic acids between two phases are of fundamental importance to understand reaction mechanisms in the biphasic systems. The distribution ratio, K_D, of each carboxylic acid (RCOOH) between xylene and water was then determined experimentally by the acid−base titration after establishing the distribution equilibrium at room temperature. We defined K_D as follows

$$K_D = [\mathrm{RCOOH}]_{\mathrm{xylene}}/[\mathrm{RCOOH}]_{\mathrm{water}} \quad (1)$$

where $[\mathrm{RCOOH}]_{\mathrm{xylene}}$ and $[\mathrm{RCOOH}]_{\mathrm{water}}$ are the concentration of the carboxylic acid in the xylene and the aqueous solution, respectively. For the measurement, an initial concentration of the respective carboxylic acids in the xylene solutions was fixed to 0.1 mol/dm^3. Results are summarized in Table 2 for benzoic, heptanoic, decanoic, and dodecanoic acid, together with their acid dissociation constants, pK_a, found in the literature. It is read that both the K_D and the p*K*a values increase with increasing number of carbon in the carboxylic acids. According to eq 1, the increased K_D values mean that the longer chain carboxylic acid prefers staying in the xylene solution to being transferred to the aqueous phase. Then the concentration of the carboxylate ions in the final aqueous solutions is reduced considerably as the carbon number in the carboxylic acids increases. Therefore, the concentration of the carboxylic acids in the initial xylene solution should be increased to provide more of them in the final aqueous solution.[15]

Effects of the initial concentrations of the carboxylic acids were then examined in terms of the distinction of solid phases obtained. Results are also listed in Table 2. For decanoic and dodecanoic acid with the larger carbon number, we actually need to increase the concentration of the carboxylic acids in the initial xylene phase ($[\mathrm{RCOOH}]_{\mathrm{xylene}} \geq 0.3$ mol/dm^{-3}) in order to obtain the LBZS ($Zn(OH)_x(RCOO)_{2-x}\cdot mH_2O$) materials. The carbonate ions from the thermal decomposition of urea and the carboxylate ions delivered from the xylene phase compete against each other in the aqueous solution as the intercalated species. In fact, at lower concentrations of decanoic and dodecanoic acid in the initial xylene solution ($[\mathrm{RCOOH}]_{\mathrm{xylene}} < 0.3$ mol/dm^3), a main product obtained in the biphasic systems was identified as zinc carbonate hydroxide hydrate ($Zn_4CO_3(OH)_6\cdot H_2O$, ICDD 11-0287) by XRD analysis. As for benzoic and heptanoic acids of the smaller carbon number, zinc carboxylate ($Zn(RCOO)_2$) was directly precipitated in the xylene phase at higher concentration of the carboxylic acids in the initial xylene phase. It was also observed for decanoic ($[\mathrm{RCOOH}]_{\mathrm{xylene}} \geq 0.4$ mol/dm^3) and dodecanoic acids ($[\mathrm{RCOOH}]_{\mathrm{xylene}} \geq 0.1$ mol/dm^3) that zinc carboxylates were crystallized in the xylene phase after cooling the biphasically separated xylene−water solutions from 80 °C to room temperature. It is therefore necessary to adjust the concentrations of the carboxylic acids properly for obtaining the LBZS compounds.

Modulation of Layered Structures. The crystal structure of the LBZSs synthesized based on the liquid−liquid biphasic systems is discussed here in terms of the molecular structure of the carboxylic acids employed. The basal spacings of the LBZSs determined from the XRD patterns (26.2, 30.2, 25.3, and 29.7 Å for the benzoate, heptanoate, decanoate, and dodecanoate, respectively) are not necessarily proportional to the molecular length of the respective carboxylic acids listed in Table 3. In particular, the basal spacings of 26.2 and 30.2 Å for the benzoate and heptanoate, respectively, have not been reported so far and are much larger than those of the LBZSs synthesized with other methods using the single-phase media (18.5−19.5 and 23.1 Å for

Table 2. Characteristic Values (K_D and pK_a) for the Carboxylic Acids Employed and the Main Products Obtained in the Biphasic Systems with Various [RCOOH] in the Initial Xylene Solutions[a]

			[RCOOH] in the initial xylene solution/mol·dm^{-3}					
carboxylic acid	K_D	pK_a	0.1	0.2	0.3	0.4	0.5	0.6
benzoic acid	8.42	4.20	LBZS	LBZS	LBZS	*ZC*	*ZC*	*ZC*
heptanoic acid	61.5	4.66	LBZS	LBZS	*ZC*	*ZC*	*ZC*	*ZC*
decanoic acid	165	4.90	*ZCHH*	*ZCHH*	LBZS	LBZS	LBZS	LBZS
dodecanoic acid	768	5.02	*ZCHH*	*ZCHH*	LBZS	LBZS	LBZS	LBZS

[a] *ZC*: Zinc carboxylate ($Zn(RCOO)_2$). *ZCHH*: Zinc carbonate hydroxide hydrate ($Zn_4CO_3(OH)_6 \cdot H_2O$).

Table 3. Molecular Length of the Carboxylic Acids and the Interlayer Basal Spacings (d_{int}) of the LBZS Compounds Intercalated with the Respective Carboxylate Ions

carboxylic acid	molecular length[a]/Å	d_{int}/Å (exclusively in the biphasic system)	d_{int}/Å (both in the biphasic and the single-phase system)
benzoic acid	5.4	26.2	19.5
heptanoic acid	8.5	30.2	23.1
decanoic acid	12.2	36.3	25.3
dodecanoic acid	14.9		29.7

[a] Distance between the carbonyl carbon and the furthest hydrogen.

the benzoate[14,17,23] and heptanoate,[16] respectively). In our report for the benzoate, we considered incorporation of an intermediate zinc hydroxide layer shifted along the [110] direction between the ordered zinc hydroxide layers to explain the discrepancy.[15] In contrast, the LBZSs with basal spacings of 25.3 and 29.7 Å for the decanoate and dodecanoate, respectively, are analogous to those synthesized with other methods (28.0 and 29.4−29.8 Å for the decanoate[20] and dodecanoate,[14,17] respectively). Our motivation of the present study was partly in building flexibly the crystal structure of the LBZSs in the liquid−liquid biphasic systems by adjusting the condition of the solid formation reaction. Below we focused on the LBZSs intercalated with the benzoate ion of the smaller carbon number and the decanoate ion of the larger one for discussing the structural flexibility.

For the benzoate, when the reaction temperature was decreased from 80 to 70 °C, another kind of LBZB (benzoate) with a basal spacing of 19.5 Å was precipitated after 24 h. As shown in Figure 6a, an XRD pattern of this LBZB exhibits equally spaced peaks with d values of 19.50 ($2\theta = 4.53°$), 9.15 (9.66°), and 13.79 (6.42°) which are indexed as (00l) planes. A peak at 2.72 Å (2θ = 32.89°) is attributed to the (100) plane, accompanied by a new shoulder peak at 2.66 Å (33.61°). The peak at 2.66 Å is not observed in the XRD pattern of the LBZB with a basal spacing of 26.2 Å that was synthesized at 80 °C for 24 h (see Figure 1). According to the TG-DTA analysis (Figure 3a and 6b), a temperature for dehydration of the zinc hydroxide layers in the "19.5 Å LBZB phase" (149 °C) is lower than that in the "26.2 Å LBZB phase" (203 °C). An approximate chemical composition of the 19.5 Å LBZB phase was determined to be $Zn(OH)_{1.43}(C_6H_5COO)_{0.57} \cdot 0.38H_2O$ based on the XRD, FT-IR (not shown), and TG-DTA results. Note that the $OH^-/C_6H_5COO^-$ ratio in the chemical composition of the 19.5 Å LBZB phase is lower than that of the 26.2 Å LBZB phase. Thus, LBZB compounds with a different crystal structure and composition

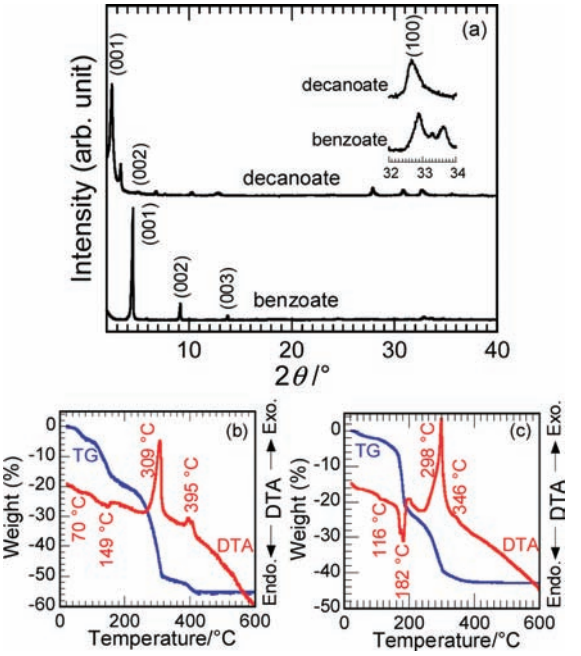

Figure 6. (a) XRD patterns and (b and c) TG-DTA curves for the LBZSs intercalated with (b) benzoate (synthesized at 70 °C for 24 h) and (c) decanoate ions (obtained at $[Zn^{2+}] = 0.2$ mol/dm^3 in the initial aqueous solution).

can be obtained by decreasing the temperature, which would lower the release rate of OH^- from urea and hence the pH value in the aqueous solution.

For the decanoate, when the concentration of Zn^{2+} in the initial aqueous solution was increased from 0.1 to 0.2 mol/dm^3, another LBZD (decanoate) with a basal spacing of 36.3 Å was formed. An XRD pattern of this LBZD shows intense peaks with d values of 36.28 ($2\theta = 2.44°$) and 18.14 Å (4.87°) in the lower 2θ range indexed as (00l) planes (Figure 6a). A single (100) diffraction peak also appears at 2.74 Å ($2\theta = 32.67°$) without any shoulder peak in the higher 2θ range. This observation is different from that for the LBZD with a basal spacing of 25.3 Å (Figure 1). In TG-DTA curves of the "36.3 Å LBZD phase" (Figure 6c), a weight loss arising from dehydration of the zinc hydroxide layers with an endothermic peak around 182 °C is not divided, which is not the case with the "25.3 Å LBZD phase" (Figure 3c). An approximate chemical composition of the 36.3 Å LBZD phase was determined to be $Zn(OH)_{1.83}(C_9H_{19}COO)_{0.17} \cdot 0.15H_2O$. It is noteworthy that the $OH^-/C_9H_{19}COO^-$ ratio in the chemical composition of the 36.3 Å LBZD phase is larger than that of the 25.3 Å LBZD phase. This suggests that LBZD

dx.doi.org/10.1021/ic1025729 |*Inorg. Chem.* 2011, 50, 3605–3612

Table 4. Synthesis Conditions, Composition ($OH^-/RCOO^-$ ratio), Interlayer Basal Spacings (d_{int}), and Dehydration (from $Zn(OH)_x$ to ZnO) Temperature of the LBZS Compounds Intercalated with the Benzoate and the Decanoate Ions

carboxylic acid	reaction temp./°C	Zn^{2+} concentration/ mol·dm^{-3}	$OH^-/RCOO^-$ ratio	d_{int}/Å	dehydration temp./°C
benzoic acid	80	0.1	6.69	26.2	203
benzoic acid	70	0.1	2.51	19.5	149
decanoic acid	80	0.2	10.8	36.3	182
decanoic acid	80	0.1	3.76	25.3	122, 170

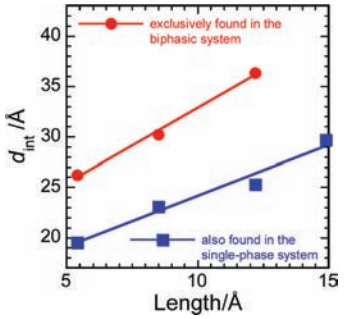

Figure 7. Interlayer spacing (d_{int}) of the LBZS compounds obtained exclusively in the biphasic system and in both the biphasic and the single-phase system, plotted against the molecular length of the intercalated carboxylate ions.

compounds with a different crystal structure and composition can be obtained by increasing the concentration of Zn^{2+} which is the building block for LBZD.

On the basis of the XRD and TG-DTA results, the LBZS compounds with different interlayer spacings (d_{int}) can be classified into two groups: one is those exclusively found in the present biphasic systems, and the other is those obtained in both the present biphasic and the previously reported single-phase systems, as listed in Tables 3 and 4. As depicted in Figure 7, the basal spacings of the LBZS compounds increase linearly in accordance with the molecular length in both groups. The LBZSs synthesized exclusively in the biphasic systems are crystallized under the higher concentration of the building blocks (Zn^{2+} and OH^-) of the zinc hydroxide layers in the aqueous phase, as read from Table 4. As a result, the $OH^-/RCOO^-$ ratios in the chemical compositions of such LBZSs are higher than those of the LBZSs obtained in both the biphasic and the single-phase systems. Since the higher $OH^-/RCOO^-$ ratio gives the unexpected larger basal spacing, the crystal structure of such LBZSs should be explained by the proposed model[15] with the presence of the intermediate layer between the ordered brucite-type layers. Figure 8 shows the crystal structure of the 36.3 and the 25.3 Å LBZD (decanoate) phase. The 36.3 Å LBZD phase has a shorter interlayer distance (18.15 Å) than that of the 25.3 Å LBZD phase due to the presence of the intermediate layer shifted along the [110] direction. This structure is unique in the LBZSs synthesized in the biphasic systems where continuous release of OH^- by decomposition of urea occurs in the aqueous phase and the continuous transport

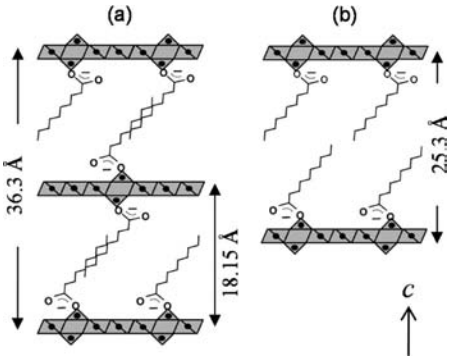

Figure 8. Crystal structure proposed for the (a) 36.3 and (b) 25.3 Å LBZD (decanoate) phase. The *c* axis is perpendicular to the zinc hydroxide layers.

of the smaller amounts of the carboxylic acids is attained from xylene to water to promote crystallization.

The LBZS compounds obtained in both the biphasic and the single-phase systems have a different crystal structure model from the intermediate layer. Such LBZSs exhibit the smaller basal spacings and the shoulder peaks for the (100) plane in their XRD patterns. As mentioned above, the weight losses caused by dehydration of the zinc hydroxide layers were divided with the corresponding endothermic peaks in the TG-DTA curves for the decanoate (Figure 3c) and dodecanoate (Figure 3d). These results can be interpreted as follows. The typical LBZSs consist of the brucite-type zinc hydroxide layers with edge-sharing octahedra.[24] One-quarter of the octahedral zinc ion sites are vacant, and two zinc ions occupy tetrahedral sites located above and below the empty octahedral sites. Water molecules coordinate to the fourth corners of the tetrahedron in place of hydroxide ions. Since the resultant complex sheet ($[Zn^{oct}_3(OH)_8Zn^{tetr}_2(H_2O)_2]^{2+}$) is positively charged, water molecules can be replaced by anions in the interlayer space to balance the whole charge in the LBZSs. In some cases with the carboxylate ions, incorporation of $RCOO^-$ causes disruption of the tetrahedral units,[14] resulting in partial formation of the zinc hydroxide layers composed of the edge-sharing octahedra only. As a result, two kinds of zinc hydroxide layers are present in one LBZS phase, giving the shoulder peaks of the (100) plane in the XRD patterns and the divided weight loss due to dehydration of the zinc hydroxide layers in the TG-DTA curves.

CONCLUSIONS

Layered zinc hydroxide compounds intercalated with various hydrophobic long-chain carboxylate ions were successfully synthesized based on liquid−liquid biphasic systems in one pot. Through the continuous transport of carboxylic acids from the organic phase to the aqueous phase in the biphasic system, layered basic zinc salts (LBZSs) intercalated with benzoate, heptanoate, decanoate, and dodecanoate ions were deposited in the aqueous phase as self-assembled films in high yields. Furthermore, the LBZS films having various 2D sheet-like morphologies on the glass substrate could be converted to the respective ZnO films with increased specific surface areas arising from the mesoporous structure developed by heat treatment without morphological change. Since the respective carboxylic acids have different distribution ratios between two immiscible

dx.doi.org/10.1021/ic1025729 |*Inorg. Chem.* 2011, 50, 3605–3612

liquid phases and different acid dissociation constants in the aqueous phase, the concentration of the carboxylic acids in the initial xylene phase was the most important factor to control the formation reaction of the LBZSs. Additionally, two types of crystal structures of the LBZSs were obtained in our synthesis method by adjusting the condition of the solid formation reaction. The LBZSs with the basal spacings exclusively found in the biphasic systems have an intermediate layer between the ordered zinc hydroxide layers. Our method using the liquid–liquid biphasic system is expected to be adaptable to the synthesis of layered metal hydroxide compounds containing a variety of hydrophobic organic species.

■ ASSOCIATED CONTENT

Supporting Information. XRD patterns (Figure S1) and FT-IR spectra (Figure S2) of the LBZS film samples after heating at various temperatures. This material is available free of charge via the Internet at http://pubs.acs.org.

■ AUTHOR INFORMATION

Corresponding Author
*E-mail: shinobu@applc.keio.ac.jp.

■ ACKNOWLEDGMENT

This work was supported by KAKENHI (21655078).

■ REFERENCES

(1) Meyn, M.; Beneke, K.; Lagaly, G. *Inorg. Chem.* **1993**, *32*, 1209.
(2) Marangoni, R.; Ramos, L. P.; Wypych, F. *J. Colloid Interface Sci.* **2009**, *330*, 303.
(3) Iosif, F.; Parvulescu, V. I.; Perez-Bernal, M. E.; Ruano-Casero, R. J.; Rives, V.; Kranjc, K.; Polanc, S.; Kocevar, M.; Genin, E.; Genet, J. P.; Michelet, V. *J. Mol. Catal. A.* **2007**, *276*, 34.
(4) Moujahid, E. M.; Dubois, M.; Besse, J. P.; Leroux, F. *Chem. Mater.* **2005**, *17*, 373.
(5) Ma, R.; Liu, Z.; Takada, K.; Iyi, N.; Bando, Y.; Sasaki, T. *J. Am. Chem. Soc.* **2007**, *129*, 5257.
(6) Huh, Y. D.; Kweon, S. S. *Bull. Korean Chem. Soc.* **2005**, *26*, 2054.
(7) Li, Y.; Xie, X.; Liu, J.; Cai, M.; Rogers, J.; Shen, W. *Chem. Eng. J.* **2008**, *136*, 398.
(8) Xu, R.; Zeng, H. C. *J. Phys. Chem. B* **2003**, *107*, 12643.
(9) Hosono, E.; Fujihara, S.; Kimura, T; Imai, H. *J. Colloid Interface Sci.* **2004**, *272*, 391.
(10) Laudise, R. A.; Ballman, A. A. *J. Phys. Chem.* **1960**, *64*, 688.
(11) Delaunay, J. J.; Kakoiyama, N.; Yamada, I. *Mater. Chem. Phys.* **2007**, *104*, 141.
(12) Kuo, T. J.; Lin, C. N.; Kuo, C. L.; Huang, M. H. *Chem. Mater.* **2007**, *19*, 5143.
(13) Saito, M.; Fujihara, S. *Energy Environ. Sci.* **2008**, *1*, 280.
(14) Ogata, S; Tagaya, H.; Karasu, M.; Kadokawa, J. *J. Mater. Chem.* **2000**, *10*, 321.
(15) Inoue, S.; Fujihara, S. *Langmuir* **2010**, *26*, 15938.
(16) Rocca, E.; Caillet, C.; Mesbah, A.; Francois, M.; Steinmetz, J. *Chem. Mater.* **2006**, *18*, 6186.
(17) Morioka, H.; Tagaya, H.; Karasu, M.; Kadokawa, J.; Chiba, K. *Inorg. Chem.* **1999**, *38*, 4211.
(18) Poul, L.; Jouini, N.; Fievet, F. *Chem. Mater.* **2000**, *12*, 3123.
(19) Kakiuchi, K.; Hosono, E.; Kimura, T.; Imai, H.; Fujihara, S. *J. Sol-Gel Sci. Technol.* **2006**, *39*, 63.
(20) Sofos, M.; Goldberger, J.; Stone, D. A.; Allen, J. E.; Ma, Q.; Herman, D. J.; Tsai, W.; Lauhon, L. J.; Stupp, S. I. *Nat. Mater.* **2009**, *8*, 68.
(21) Stählin, W.; Oswald, H. R. *Acta Crystallogr. B* **1970**, *26*, 860.
(22) Stoilova, D.; Koleva, V.; Vassileva, V. *Spectrochim. Acta A* **2002**, *58*, 2051.
(23) Takahashi, S.; Iwasa, T.; Kanazawa, Y.; Umetsu, Y.; Narita, E. *Nippon Kagaku Kaishi* **1997**, *7*, 502.
(24) Kasai, A.; Fujihara, S. *Inorg. Chem.* **2006**, *45*, 415.